BABAR-CONF-06/038
SLAC-PUB-12028

Measurement of the CKM angle γ in $B^{\mp} \to D^{(*)}K^{\mp}$ decays with a Dalitz analysis of $D^0 \to K^0_s\pi^-\pi^+$

The *BABAR* Collaboration

July 31, 2006

Abstract

We present a measurement of the Cabibbo-Kobayashi-Maskawa CP-violating phase γ with a Dalitz analysis of neutral D-meson decays to the $K^0_s\pi^-\pi^+$ final state from $B^{\mp} \to D^{(*)}K^{\mp}$ decays, using a sample of 347 million $B\bar{B}$ events collected by the *BABAR* detector. We measure $\gamma = (92 \pm 41 \pm 11 \pm 12)^{\circ}$, where the first error is statistical, the second is the experimental systematic uncertainty and the third reflects the Dalitz model uncertainty. For the ratios $r_B^{(*)}$ between the magnitudes of amplitudes $\mathcal{A}(B^- \to D^{(*)0}K^-)$ and $\mathcal{A}(B^- \to \bar{D}^{(*)0}K^-)$ we obtain the one-standard deviation intervals $[0, 0.14]$ and $[0.02, 0.20]$, respectively. All results presented here are preliminary.

Submitted to the 33rd International Conference on High-Energy Physics, ICHEP 06, 26 July—2 August 2006, Moscow, Russia.

Stanford Linear Accelerator Center, Stanford University, Stanford, CA 94309

Work supported in part by Department of Energy contract DE-AC03-76SF00515.

The *BABAR* Collaboration,

B. Aubert, R. Barate, M. Bona, D. Boutigny, F. Couderc, Y. Karyotakis, J. P. Lees, V. Poireau, V. Tisserand, A. Zghiche

Laboratoire de Physique des Particules, IN2P3/CNRS et Université de Savoie, F-74941 Annecy-Le-Vieux, France

E. Grauges

Universitat de Barcelona, Facultat de Fisica, Departament ECM, E-08028 Barcelona, Spain

A. Palano

Università di Bari, Dipartimento di Fisica and INFN, I-70126 Bari, Italy

J. C. Chen, N. D. Qi, G. Rong, P. Wang, Y. S. Zhu

Institute of High Energy Physics, Beijing 100039, China

G. Eigen, I. Ofte, B. Stugu

University of Bergen, Institute of Physics, N-5007 Bergen, Norway

G. S. Abrams, M. Battaglia, D. N. Brown, J. Button-Shafer, R. N. Cahn, E. Charles, M. S. Gill, Y. Groysman, R. G. Jacobsen, J. A. Kadyk, L. T. Kerth, Yu. G. Kolomensky, G. Kukartsev, G. Lynch, L. M. Mir, T. J. Orimoto, M. Pripstein, N. A. Roe, M. T. Ronan, W. A. Wenzel

Lawrence Berkeley National Laboratory and University of California, Berkeley, California 94720, USA

P. del Amo Sanchez, M. Barrett, K. E. Ford, A. J. Hart, T. J. Harrison, C. M. Hawkes, S. E. Morgan, A. T. Watson

University of Birmingham, Birmingham, B15 2TT, United Kingdom

T. Held, H. Koch, B. Lewandowski, M. Pelizaeus, K. Peters, T. Schroeder, M. Steinke

Ruhr Universität Bochum, Institut für Experimentalphysik 1, D-44780 Bochum, Germany

J. T. Boyd, J. P. Burke, W. N. Cottingham, D. Walker

University of Bristol, Bristol BS8 1TL, United Kingdom

D. J. Asgeirsson, T. Cuhadar-Donszelmann, B. G. Fulsom, C. Hearty, N. S. Knecht, T. S. Mattison, J. A. McKenna

University of British Columbia, Vancouver, British Columbia, Canada V6T 1Z1

A. Khan, P. Kyberd, M. Saleem, D. J. Sherwood, L. Teodorescu

Brunel University, Uxbridge, Middlesex UB8 3PH, United Kingdom

V. E. Blinov, A. D. Bukin, V. P. Druzhinin, V. B. Golubev, A. P. Onuchin, S. I. Serednyakov, Yu. I. Skovpen, E. P. Solodov, K. Yu Todyshev

Budker Institute of Nuclear Physics, Novosibirsk 630090, Russia

D. S. Best, M. Bondioli, M. Bruinsma, M. Chao, S. Curry, I. Eschrich, D. Kirkby, A. J. Lankford, P. Lund, M. Mandelkern, R. K. Mommsen, W. Roethel, D. P. Stoker

University of California at Irvine, Irvine, California 92697, USA

S. Abachi, C. Buchanan

University of California at Los Angeles, Los Angeles, California 90024, USA

S. D. Foulkes, J. W. Gary, O. Long, B. C. Shen, K. Wang, L. Zhang
University of California at Riverside, Riverside, California 92521, USA

H. K. Hadavand, E. J. Hill, H. P. Paar, S. Rahatlou, V. Sharma
University of California at San Diego, La Jolla, California 92093, USA

J. W. Berryhill, C. Campagnari, A. Cunha, B. Dahmes, T. M. Hong, D. Kovalskyi, J. D. Richman
University of California at Santa Barbara, Santa Barbara, California 93106, USA

T. W. Beck, A. M. Eisner, C. J. Flacco, C. A. Heusch, J. Kroseberg, W. S. Lockman, G. Nesom, T. Schalk, B. A. Schumm, A. Seiden, P. Spradlin, D. C. Williams, M. G. Wilson
University of California at Santa Cruz, Institute for Particle Physics, Santa Cruz, California 95064, USA

J. Albert, E. Chen, A. Dvoretskii, F. Fang, D. G. Hitlin, I. Narsky, T. Piatenko, F. C. Porter, A. Ryd, A. Samuel
California Institute of Technology, Pasadena, California 91125, USA

G. Mancinelli, B. T. Meadows, K. Mishra, M. D. Sokoloff
University of Cincinnati, Cincinnati, Ohio 45221, USA

F. Blanc, P. C. Bloom, S. Chen, W. T. Ford, J. F. Hirschauer, A. Kreisel, M. Nagel, U. Nauenberg, A. Olivas, W. O. Ruddick, J. G. Smith, K. A. Ulmer, S. R. Wagner, J. Zhang
University of Colorado, Boulder, Colorado 80309, USA

A. Chen, E. A. Eckhart, A. Soffer, W. H. Toki, R. J. Wilson, F. Winklmeier, Q. Zeng
Colorado State University, Fort Collins, Colorado 80523, USA

D. D. Altenburg, E. Feltresi, A. Hauke, H. Jasper, J. Merkel, A. Petzold, B. Spaan
Universität Dortmund, Institut für Physik, D-44221 Dortmund, Germany

T. Brandt, V. Klose, H. M. Lacker, W. F. Mader, R. Nogowski, J. Schubert, K. R. Schubert, R. Schwierz, J. E. Sundermann, A. Volk
Technische Universität Dresden, Institut für Kern- und Teilchenphysik, D-01062 Dresden, Germany

D. Bernard, G. R. Bonneaud, E. Latour, Ch. Thiebaux, M. Verderi
Laboratoire Leprince-Ringuet, CNRS/IN2P3, Ecole Polytechnique, F-91128 Palaiseau, France

P. J. Clark, W. Gradl, F. Muheim, S. Playfer, A. I. Robertson, Y. Xie
University of Edinburgh, Edinburgh EH9 3JZ, United Kingdom

M. Andreotti, D. Bettoni, C. Bozzi, R. Calabrese, G. Cibinetto, E. Luppi, M. Negrini, A. Petrella, L. Piemontese, E. Prencipe
Università di Ferrara, Dipartimento di Fisica and INFN, I-44100 Ferrara, Italy

F. Anulli, R. Baldini-Ferroli, A. Calcaterra, R. de Sangro, G. Finocchiaro, S. Pacetti, P. Patteri, I. M. Peruzzi,[1] M. Piccolo, M. Rama, A. Zallo
Laboratori Nazionali di Frascati dell'INFN, I-00044 Frascati, Italy

[1]Also with Università di Perugia, Dipartimento di Fisica, Perugia, Italy

A. Buzzo, R. Capra, R. Contri, M. Lo Vetere, M. M. Macri, M. R. Monge, S. Passaggio, C. Patrignani, E. Robutti, A. Santroni, S. Tosi

Università di Genova, Dipartimento di Fisica and INFN, I-16146 Genova, Italy

G. Brandenburg, K. S. Chaisanguanthum, M. Morii, J. Wu

Harvard University, Cambridge, Massachusetts 02138, USA

R. S. Dubitzky, J. Marks, S. Schenk, U. Uwer

Universität Heidelberg, Physikalisches Institut, Philosophenweg 12, D-69120 Heidelberg, Germany

D. J. Bard, W. Bhimji, D. A. Bowerman, P. D. Dauncey, U. Egede, R. L. Flack, J. A. Nash, M. B. Nikolich, W. Panduro Vazquez

Imperial College London, London, SW7 2AZ, United Kingdom

P. K. Behera, X. Chai, M. J. Charles, U. Mallik, N. T. Meyer, V. Ziegler

University of Iowa, Iowa City, Iowa 52242, USA

J. Cochran, H. B. Crawley, L. Dong, V. Eyges, W. T. Meyer, S. Prell, E. I. Rosenberg, A. E. Rubin

Iowa State University, Ames, Iowa 50011-3160, USA

A. V. Gritsan

Johns Hopkins University, Baltimore, Maryland 21218, USA

A. G. Denig, M. Fritsch, G. Schott

Universität Karlsruhe, Institut für Experimentelle Kernphysik, D-76021 Karlsruhe, Germany

N. Arnaud, M. Davier, G. Grosdidier, A. Höcker, F. Le Diberder, V. Lepeltier, A. M. Lutz, A. Oyanguren, S. Pruvot, S. Rodier, P. Roudeau, M. H. Schune, A. Stocchi, W. F. Wang, G. Wormser

Laboratoire de l'Accélérateur Linéaire, IN2P3/CNRS et Université Paris-Sud 11, Centre Scientifique d'Orsay, B.P. 34, F-91898 ORSAY Cedex, France

C. H. Cheng, D. J. Lange, D. M. Wright

Lawrence Livermore National Laboratory, Livermore, California 94550, USA

C. A. Chavez, I. J. Forster, J. R. Fry, E. Gabathuler, R. Gamet, K. A. George, D. E. Hutchcroft, D. J. Payne, K. C. Schofield, C. Touramanis

University of Liverpool, Liverpool L69 7ZE, United Kingdom

A. J. Bevan, F. Di Lodovico, W. Menges, R. Sacco

Queen Mary, University of London, E1 4NS, United Kingdom

G. Cowan, H. U. Flaecher, D. A. Hopkins, P. S. Jackson, T. R. McMahon, S. Ricciardi, F. Salvatore, A. C. Wren

University of London, Royal Holloway and Bedford New College, Egham, Surrey TW20 0EX, United Kingdom

D. N. Brown, C. L. Davis

University of Louisville, Louisville, Kentucky 40292, USA

J. Allison, N. R. Barlow, R. J. Barlow, Y. M. Chia, C. L. Edgar, G. D. Lafferty, M. T. Naisbit, J. C. Williams, J. I. Yi

University of Manchester, Manchester M13 9PL, United Kingdom

C. Chen, W. D. Hulsbergen, A. Jawahery, C. K. Lae, D. A. Roberts, G. Simi

University of Maryland, College Park, Maryland 20742, USA

G. Blaylock, C. Dallapiccola, S. S. Hertzbach, X. Li, T. B. Moore, S. Saremi, H. Staengle

University of Massachusetts, Amherst, Massachusetts 01003, USA

R. Cowan, G. Sciolla, S. J. Sekula, M. Spitznagel, F. Taylor, R. K. Yamamoto

Massachusetts Institute of Technology, Laboratory for Nuclear Science, Cambridge, Massachusetts 02139, USA

H. Kim, S. E. Mclachlin, P. M. Patel, S. H. Robertson

McGill University, Montréal, Québec, Canada H3A 2T8

A. Lazzaro, V. Lombardo, F. Palombo

Università di Milano, Dipartimento di Fisica and INFN, I-20133 Milano, Italy

J. M. Bauer, L. Cremaldi, V. Eschenburg, R. Godang, R. Kroeger, D. A. Sanders, D. J. Summers, H. W. Zhao

University of Mississippi, University, Mississippi 38677, USA

S. Brunet, D. Côté, M. Simard, P. Taras, F. B. Viaud

Université de Montréal, Physique des Particules, Montréal, Québec, Canada H3C 3J7

H. Nicholson

Mount Holyoke College, South Hadley, Massachusetts 01075, USA

N. Cavallo,[2] G. De Nardo, F. Fabozzi,[3] C. Gatto, L. Lista, D. Monorchio, P. Paolucci, D. Piccolo, C. Sciacca

Università di Napoli Federico II, Dipartimento di Scienze Fisiche and INFN, I-80126, Napoli, Italy

M. A. Baak, G. Raven, H. L. Snoek

NIKHEF, National Institute for Nuclear Physics and High Energy Physics, NL-1009 DB Amsterdam, The Netherlands

C. P. Jessop, J. M. LoSecco

University of Notre Dame, Notre Dame, Indiana 46556, USA

T. Allmendinger, G. Benelli, L. A. Corwin, K. K. Gan, K. Honscheid, D. Hufnagel, P. D. Jackson, H. Kagan, R. Kass, A. M. Rahimi, J. J. Regensburger, R. Ter-Antonyan, Q. K. Wong

Ohio State University, Columbus, Ohio 43210, USA

N. L. Blount, J. Brau, R. Frey, O. Igonkina, J. A. Kolb, M. Lu, R. Rahmat, N. B. Sinev, D. Strom, J. Strube, E. Torrence

University of Oregon, Eugene, Oregon 97403, USA

[2]Also with Università della Basilicata, Potenza, Italy
[3]Also with Università della Basilicata, Potenza, Italy

A. Gaz, M. Margoni, M. Morandin, A. Pompili, M. Posocco, M. Rotondo, F. Simonetto, R. Stroili, C. Voci

Università di Padova, Dipartimento di Fisica and INFN, I-35131 Padova, Italy

M. Benayoun, H. Briand, J. Chauveau, P. David, L. Del Buono, Ch. de la Vaissière, O. Hamon, B. L. Hartfiel, M. J. J. John, Ph. Leruste, J. Malclès, J. Ocariz, L. Roos, G. Therin

Laboratoire de Physique Nucléaire et de Hautes Energies, IN2P3/CNRS, Université Pierre et Marie Curie-Paris6, Université Denis Diderot-Paris7, F-75252 Paris, France

L. Gladney, J. Panetta

University of Pennsylvania, Philadelphia, Pennsylvania 19104, USA

M. Biasini, R. Covarelli

Università di Perugia, Dipartimento di Fisica and INFN, I-06100 Perugia, Italy

C. Angelini, G. Batignani, S. Bettarini, F. Bucci, G. Calderini, M. Carpinelli, R. Cenci, F. Forti, M. A. Giorgi, A. Lusiani, G. Marchiori, M. A. Mazur, M. Morganti, N. Neri, E. Paoloni, G. Rizzo, J. J. Walsh

Università di Pisa, Dipartimento di Fisica, Scuola Normale Superiore and INFN, I-56127 Pisa, Italy

M. Haire, D. Judd, D. E. Wagoner

Prairie View A&M University, Prairie View, Texas 77446, USA

J. Biesiada, N. Danielson, P. Elmer, Y. P. Lau, C. Lu, J. Olsen, A. J. S. Smith, A. V. Telnov

Princeton University, Princeton, New Jersey 08544, USA

F. Bellini, G. Cavoto, A. D'Orazio, D. del Re, E. Di Marco, R. Faccini, F. Ferrarotto, F. Ferroni, M. Gaspero, L. Li Gioi, M. A. Mazzoni, S. Morganti, G. Piredda, F. Polci, F. Safai Tehrani, C. Voena

Università di Roma La Sapienza, Dipartimento di Fisica and INFN, I-00185 Roma, Italy

M. Ebert, H. Schröder, R. Waldi

Universität Rostock, D-18051 Rostock, Germany

T. Adye, N. De Groot, B. Franek, E. O. Olaiya, F. F. Wilson

Rutherford Appleton Laboratory, Chilton, Didcot, Oxon, OX11 0QX, United Kingdom

R. Aleksan, S. Emery, A. Gaidot, S. F. Ganzhur, G. Hamel de Monchenault, W. Kozanecki, M. Legendre, G. Vasseur, Ch. Yèche, M. Zito

DSM/Dapnia, CEA/Saclay, F-91191 Gif-sur-Yvette, France

X. R. Chen, H. Liu, W. Park, M. V. Purohit, J. R. Wilson

University of South Carolina, Columbia, South Carolina 29208, USA

M. T. Allen, D. Aston, R. Bartoldus, P. Bechtle, N. Berger, R. Claus, J. P. Coleman, M. R. Convery, M. Cristinziani, J. C. Dingfelder, J. Dorfan, G. P. Dubois-Felsmann, D. Dujmic, W. Dunwoodie, R. C. Field, T. Glanzman, S. J. Gowdy, M. T. Graham, P. Grenier,[4] V. Halyo, C. Hast, T. Hryn'ova, W. R. Innes, M. H. Kelsey, P. Kim, D. W. G. S. Leith, S. Li, S. Luitz, V. Luth, H. L. Lynch, D. B. MacFarlane, H. Marsiske, R. Messner, D. R. Muller, C. P. O'Grady, V. E. Ozcan, A. Perazzo, M. Perl, T. Pulliam, B. N. Ratcliff, A. Roodman, A. A. Salnikov, R. H. Schindler, J. Schwiening, A. Snyder, J. Stelzer, D. Su, M. K. Sullivan, K. Suzuki, S. K. Swain, J. M. Thompson, J. Va'vra, N. van

[4]Also at Laboratoire de Physique Corpusculaire, Clermont-Ferrand, France

Bakel, M. Weaver, A. J. R. Weinstein, W. J. Wisniewski, M. Wittgen, D. H. Wright, A. K. Yarritu, K. Yi, C. C. Young

Stanford Linear Accelerator Center, Stanford, California 94309, USA

P. R. Burchat, A. J. Edwards, S. A. Majewski, B. A. Petersen, C. Roat, L. Wilden

Stanford University, Stanford, California 94305-4060, USA

S. Ahmed, M. S. Alam, R. Bula, J. A. Ernst, V. Jain, B. Pan, M. A. Saeed, F. R. Wappler, S. B. Zain

State University of New York, Albany, New York 12222, USA

W. Bugg, M. Krishnamurthy, S. M. Spanier

University of Tennessee, Knoxville, Tennessee 37996, USA

R. Eckmann, J. L. Ritchie, A. Satpathy, C. J. Schilling, R. F. Schwitters

University of Texas at Austin, Austin, Texas 78712, USA

J. M. Izen, X. C. Lou, S. Ye

University of Texas at Dallas, Richardson, Texas 75083, USA

F. Bianchi, F. Gallo, D. Gamba

Università di Torino, Dipartimento di Fisica Sperimentale and INFN, I-10125 Torino, Italy

M. Bomben, L. Bosisio, C. Cartaro, F. Cossutti, G. Della Ricca, S. Dittongo, L. Lanceri, L. Vitale

Università di Trieste, Dipartimento di Fisica and INFN, I-34127 Trieste, Italy

V. Azzolini, N. Lopez-March, F. Martinez-Vidal

IFIC, Universitat de Valencia-CSIC, E-46071 Valencia, Spain

Sw. Banerjee, B. Bhuyan, C. M. Brown, D. Fortin, K. Hamano, R. Kowalewski, I. M. Nugent, J. M. Roney, R. J. Sobie

University of Victoria, Victoria, British Columbia, Canada V8W 3P6

J. J. Back, P. F. Harrison, T. E. Latham, G. B. Mohanty, M. Pappagallo

Department of Physics, University of Warwick, Coventry CV4 7AL, United Kingdom

H. R. Band, X. Chen, B. Cheng, S. Dasu, M. Datta, K. T. Flood, J. J. Hollar, P. E. Kutter, B. Mellado, A. Mihalyi, Y. Pan, M. Pierini, R. Prepost, S. L. Wu, Z. Yu

University of Wisconsin, Madison, Wisconsin 53706, USA

H. Neal

Yale University, New Haven, Connecticut 06511, USA

1 INTRODUCTION

The angle γ of the unitarity triangle is the phase of the Cabibbo-Kobayashi-Maskawa (CKM) matrix [1] defined as $\gamma \equiv \arg\left[-V_{ud}V_{ub}^*/V_{cd}V_{cb}^*\right]$, which corresponds to the phase of the element V_{ub}^*, i.e. $V_{ub} = |V_{ub}|e^{-i\gamma}$, in the Wolfenstein parameterization [2]. Various methods have been proposed to extract γ using $B^\mp \to \tilde{D}^0 K^\mp$ decays, all exploiting the interference between the color allowed $B^- \to D^0 K^-$ ($b \to \overline{u}s \propto V_{cb}$) and the color suppressed $B^- \to \bar{D}^0 K^-$ ($b \to u\overline{c}s \propto V_{ub}$) transitions [3], when the D^0 and $\bar{D}^0$ are reconstructed in a common final state [4, 5, 6, 7]. The symbol $\tilde{D}^0$ indicates either a D^0 or a $\bar{D}^0$ meson. The extraction of γ with these decays is theoretically clean because the main contributions to the amplitudes come from tree-level diagrams (see Fig. 1).

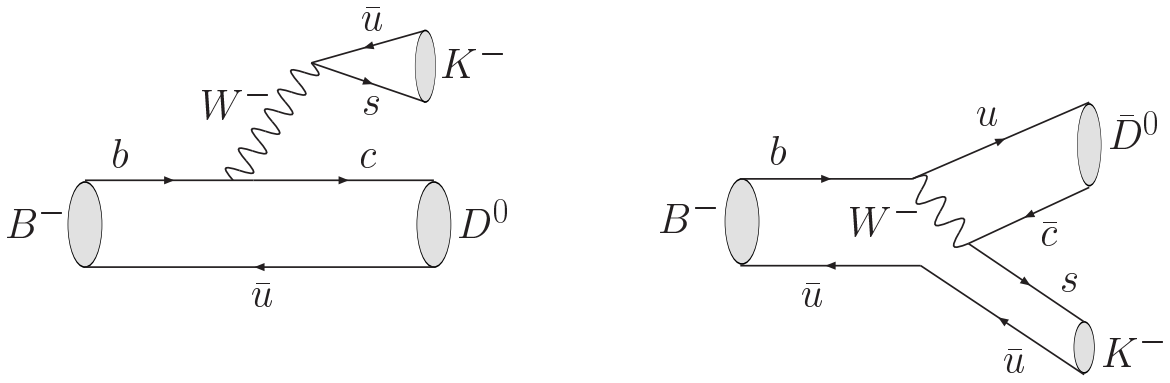

Figure 1: Diagrams contributing to $B^- \to \tilde{D}^0 K^-$ decay. The left diagram proceeds via $b \to \overline{u}s$ transition, while the right diagram proceeds via $b \to u\overline{c}s$ transition and is color suppressed.

Both *BABAR* [8, 9] and Belle [10] have reported on a measurement of γ based on $B^- \to \tilde{D}^{(*)0} K^-$ and $B^- \to \tilde{D}^0 K^{*-}$ decays with a Dalitz analysis of $\tilde{D}^0 \to K^0_S\pi^-\pi^+$, with $D^{*0} \to D^0\pi^0$ and $D^{*0} \to D^0\gamma$ (*BABAR* only), and $K^{*-} \to K^0_S\pi^-$. In this paper we report on an update with $B^- \to \tilde{D}^{(*)0} K^-$ decays.

Assuming no *CP* asymmetry in D^0 decays, the $B^\mp \to \tilde{D}^{(*)0} K^\mp$, $\tilde{D}^{*0} \to \tilde{D}^0\pi^0, \tilde{D}^0\gamma$, $\tilde{D}^0 \to K^0_S\pi^-\pi^+$ decay chain rate $\Gamma^{(*)}_\mp(m^2_-, m^2_+)$ can be written as [6]

$$\begin{aligned}\Gamma^{(*)}_\mp(m^2_-, m^2_+) \;\propto\; & |\mathcal{A}_{D\mp}|^2 + {r_B^{(*)}}^2 |\mathcal{A}_{D\pm}|^2 + \\ & 2kr_B^{(*)} \left\{\cos(\delta_B^{(*)} \mp \gamma)\,\mathrm{Re}[\mathcal{A}_{D\mp}\mathcal{A}^*_{D\pm}] + \sin(\delta_B^{(*)} \mp \gamma)\,\mathrm{Im}[\mathcal{A}_{D\mp}\mathcal{A}^*_{D\pm}]\right\}\,, \quad (1)\end{aligned}$$

where m^2_- and m^2_+ are the squared invariant masses of the $K^0_S\pi^-$ and $K^0_S\pi^+$ combinations, respectively, and $\mathcal{A}_{D\mp} \equiv \mathcal{A}_D(m^2_\mp, m^2_\pm)$, with $\mathcal{A}_{D-}$ ($\mathcal{A}_{D+}$) the amplitude of the $D^0 \to K^0_S\pi^-\pi^+$ ($\overline{D}^0 \to K^0_S\pi^+\pi^-$) decay. The value of the *CP*-odd phase γ changes sign for B^+ and B^- in Eq. (1), leading to different rates in corresponding regions of the D^0 Dalitz plane, for B^+ and B^- decays. We introduce here the *CP (cartesian) parameters* $x^{(*)}_\mp$ and $y^{(*)}_\mp$ [8], defined respectively as the real and imaginary part of $r_B^{(*)} e^{i(\delta_B^{(*)} \mp \gamma)}$, for which the constraint ${r_B^{(*)}}^2 = {x^{(*)}_\mp}^2 + {y^{(*)}_\mp}^2$ holds. Here, $r_B^{(*)}$ is the magnitude of the ratio of the amplitudes $\mathcal{A}(B^- \to \bar{D}^{(*)0} K^-)$ and $\mathcal{A}(B^- \to D^{(*)0} K^-)$ and $\delta_B^{(*)}$ is their relative strong phase. As a consequence of parity and angular momentum conservation in the

$\tilde{D}^{(*)0}$ decay, the factor k in Eq. (1) takes the value $+1$ for $B^{\mp} \to \tilde{D}^0 K^{\mp}$ and $B^{\mp} \to \tilde{D}^{*0}(\tilde{D}^0\pi^0)K^{\mp}$, and -1 for $B^{\mp} \to \tilde{D}^{*0}(\tilde{D}^0\gamma)K^{\mp}$ [11].

Once the decay amplitude $\mathcal{A}_D$ is known, the Dalitz plot distributions for $\tilde{D}^0$ from $B^- \to \tilde{D}^{(*)0}K^-$ and $B^+ \to \tilde{D}^{(*)0}K^+$ decays can be simultaneously fitted to $\Gamma_-^{(*)}(m_-^2, m_+^2)$ and $\Gamma_+^{(*)}(m_-^2, m_+^2)$ as given by Eq. (1), respectively. A maximum likelihood technique is used to measure the *CP*-violating parameters $x_{\mp}^{(*)}$, $y_{\mp}^{(*)}$. From them, confidence regions for γ, $r_B^{(*)}$ and $\delta_B^{(*)}$ are obtained with a frequentist method. We extract $x_{\mp}^{(*)}$, $y_{\mp}^{(*)}$ instead of $\gamma, \delta_B^{(*)}, r_B^{(*)}$ because the distributions of the cartesian parameters are unbiased and Gaussian, while the distributions of $\gamma, \delta_B^{(*)}, r_B^{(*)}$ don't have these properties for small values of $r_B^{(*)}$ and low-statistics samples.

2 THE *BABAR* DETECTOR AND DATASET

The analysis is based on a sample of approximately 347 million $B\overline{B}$ pairs collected by the *BABAR* detector at the SLAC PEP-II e^+e^- asymmetric-energy storage ring. The *BABAR* detector is optimized for the asymmetric-energy beams at PEP-II and is described in [12]. We summarize briefly the components that are crucial to this analysis. Charged-particle tracking is provided by a five-layer silicon vertex tracker (SVT) and a 40-layer drift chamber (DCH). In addition to providing precise space coordinates for tracking, the SVT and DCH also measure the specific ionization (dE/dx), which is used for particle identification of low-momentum charged particles. At higher momenta ($p > 0.7$ GeV/c) pions and kaons are identified by Cherenkov radiation detected in a ring-imaging device (DIRC). The typical separation between pions and kaons varies from 8σ at 2 GeV/c to 2.5σ at 4 GeV/c. The position and energy of photons are measured with an electromagnetic calorimeter (EMC) consisting of 6580 thallium-doped CsI crystals. These systems are mounted inside a 1.5 T solenoidal super-conducting magnet.

3 EVENT SELECTION

We reconstruct the $B^- \to \tilde{D}^{(*)0}K^-$ decays with $\tilde{D}^{(*)0} \to \tilde{D}^0\pi^0, \tilde{D}^0\gamma$ and $\tilde{D}^0 \to K_S^0\pi^-\pi^+$ [3]. The K_S^0 candidates are formed from oppositely charged pions with a reconstructed invariant mass within 9 MeV/c^2 of the nominal K_S^0 mass [13]. The two pions are constrained to originate from the same point. The $\tilde{D}^0 \to K_S^0\pi^-\pi^+$ candidates are selected by combining mass constrained K_S^0 candidates with two oppositely charged pions having an invariant mass within 12 MeV/c^2 of the nominal D^0 mass [13]. The π^0 candidates from $D^{*0} \to D^0\pi^0$ are formed from pairs of photons with invariant mass in the range $[115, 150]$ MeV/c^2, and with photon energy greater than 30 MeV. Photon candidates from $D^{*0} \to D^0\gamma$ are selected if their energy is greater than 100 MeV. $D^{*0} \to D^0\pi^0(D^0\gamma)$ candidates are required to have a D^{*0}-D^0 mass difference within 2.5 (10) MeV/c^2 of its nominal value [13], corresponding to about two standard deviations. $B^- \to \tilde{D}^{(*)0}K^-$ candidates are formed by combining a $\tilde{D}^{(*)0}$ candidate with a track identified as a kaon.

We select B mesons by using the energy difference $\Delta E = E_B^* - E_i^*/2$, and the beam-energy substituted mass, $m_{\rm ES} = \sqrt{(E_i^{*2}/2 + \mathbf{p_i}\cdot\mathbf{p_B})^2/E_i^2 - p_B^2}$, where the subscripts i and B refer to the initial e^+e^- system and the B candidate, respectively, and the asterisk denotes the center-of-mass (CM) frame. The resolution of ΔE ranges between 15 MeV and 18 MeV depending on the decay mode. The resolution of $m_{\rm ES}$ is about 2.6 MeV/c^2 for all the B decay modes. We define a selection region through the requirement $-80 < \Delta E < 120$ MeV and $m_{\rm ES} > 5.2$ GeV/c^2.

To suppress $e^+e^- \to q\bar{q}$, $q = u, d, s, c$ (continuum) events, we require $|\cos\theta_T| < 0.8$ where θ_T is defined as the angle between the thrust axis of the B candidate and that of the rest of the event. Furthermore we define a Fisher discriminant $\mathcal{F}$ that we use in a likelihood fit to separate continuum and $B\overline{B}$ events. It is defined as a linear combination of four topological variables: $L_0 = \sum_i p_i^*$, $L_2 = \sum_i p_i^* |\cos\theta_i^*|^2$, the absolute value of the cosine of the CM polar angle of the B candidate momentum, and $|\cos\theta_T|$. Here, p_i^* and θ_i^* are the CM momentum and the angle of the remaining tracks and clusters in the event, with respect to the B candidate thrust axis. If both $B^- \to \tilde{D}^{*0}(\tilde{D}^0\pi^0)K^-$ and $B^- \to \tilde{D}^{*0}(\tilde{D}^0\gamma)K^-$ candidates are selected in the same event, only the $B^- \to \tilde{D}^{*0}(\tilde{D}^0\pi^0)K^-$ is kept. The cross-feed among the different samples is negligible except for $B^- \to \tilde{D}^{*0}(\tilde{D}^0\gamma)K^-$, where the background from $B^- \to \tilde{D}^{*0}(\tilde{D}^0\pi^0)K^-$ is about 5% of the signal yield. This contamination has a negligible effect on the measurement of the *CP* parameters.

The reconstruction efficiencies are 15%, 7%, 9%, for the $B^- \to \tilde{D}^0K^-$, $B^- \to \tilde{D}^{*0}(\tilde{D}^0\pi^0)K^-$ and $B^- \to \tilde{D}^{*0}(\tilde{D}^0\gamma)K^-$ decay modes, respectively. Fig. 2 shows the $m_{\rm ES}$ distributions after all selection criteria plus a tighter requirement on ΔE, $|\Delta E| < 30$ MeV, are applied. The largest background contribution is from continuum events or $B\overline{B}$ decays where a fake or true D^0 is combined with a random track. Another source of background is given by those $B^- \to D^{(*)0}\pi^-$ decays where the prompt pion is misidentified as kaon. These decays are separated from the signal using their different ΔE distribution.

4 The $D^0 \to K^0_S\pi^-\pi^+$ DECAY MODEL

The $D^0 \to K^0_S\pi^-\pi^+$ decay amplitude $\mathcal{A}_D(m_-^2, m_+^2)$ is determined from an unbinned maximum-likelihood fit to the Dalitz plot distribution of a high-purity (97.7%) D^0 sample from 390328 $D^{*+} \to D^0\pi^+$ decays reconstructed in 270 fb^{-1} of data, shown in Fig. 3. Our reference model to describe $\mathcal{A}_D(m_-^2, m_+^2)$ is based on Breit-Wigner (BW) parameterizations of a set of resonances, and is the same as used for our previously reported measurement of γ on $B^- \to \tilde{D}^{(*)0}K^-$, $B^- \to \tilde{D}^0K^{*-}$, $\tilde{D}^0 \to K^0_S\pi^-\pi^+$ decays [8, 9].

The decay amplitude in the reference model is expressed as a sum of two-body decay-matrix elements (subscript r) and a non-resonant (subscript NR) contribution,

$$\mathcal{A}_D(m_-^2, m_+^2) = \Sigma_r a_r e^{i\phi_r}\mathcal{A}_r(m_-^2, m_+^2) + a_{\rm NR}e^{i\phi_{\rm NR}} \ , \qquad (2)$$

where each term is parameterized with an amplitude a_r ($a_{\rm NR}$) and a phase ϕ_r ($\phi_{\rm NR}$). The function $\mathcal{A}_r(m_-^2, m_+^2)$ is the Lorentz-invariant expression for the matrix element of a D^0 meson decaying into $K^0_S\pi^-\pi^+$ through an intermediate resonance r, parameterized as a function of position in the Dalitz plane. For $r = \rho(770)$ and $\rho(1450)$ we use the functional form suggested in Ref. [14], while the remaining resonances are parameterized by a spin-dependent relativistic BW distribution. The angular dependence of the BW terms is described with the helicity formalism as shown in [15][5]. Mass and width values are taken from [13], with the exception of $K_0^*(1430)^+$ taken from [16]. The model consists of 13 resonances leading to 16 two-body decay amplitudes and phases (see Table 1), plus the non-resonant contribution, and accounts for efficiency variations across the Dalitz plane and the small background contribution. All the resonances considered in this model are well established except for the two scalar $\pi\pi$ resonances, σ and σ', whose masses and widths are obtained from our sample [17]. Their addition to the model is motivated by an improvement in the description of the data.

[5]The label A and B should be swapped in Eq. (6) of [15].

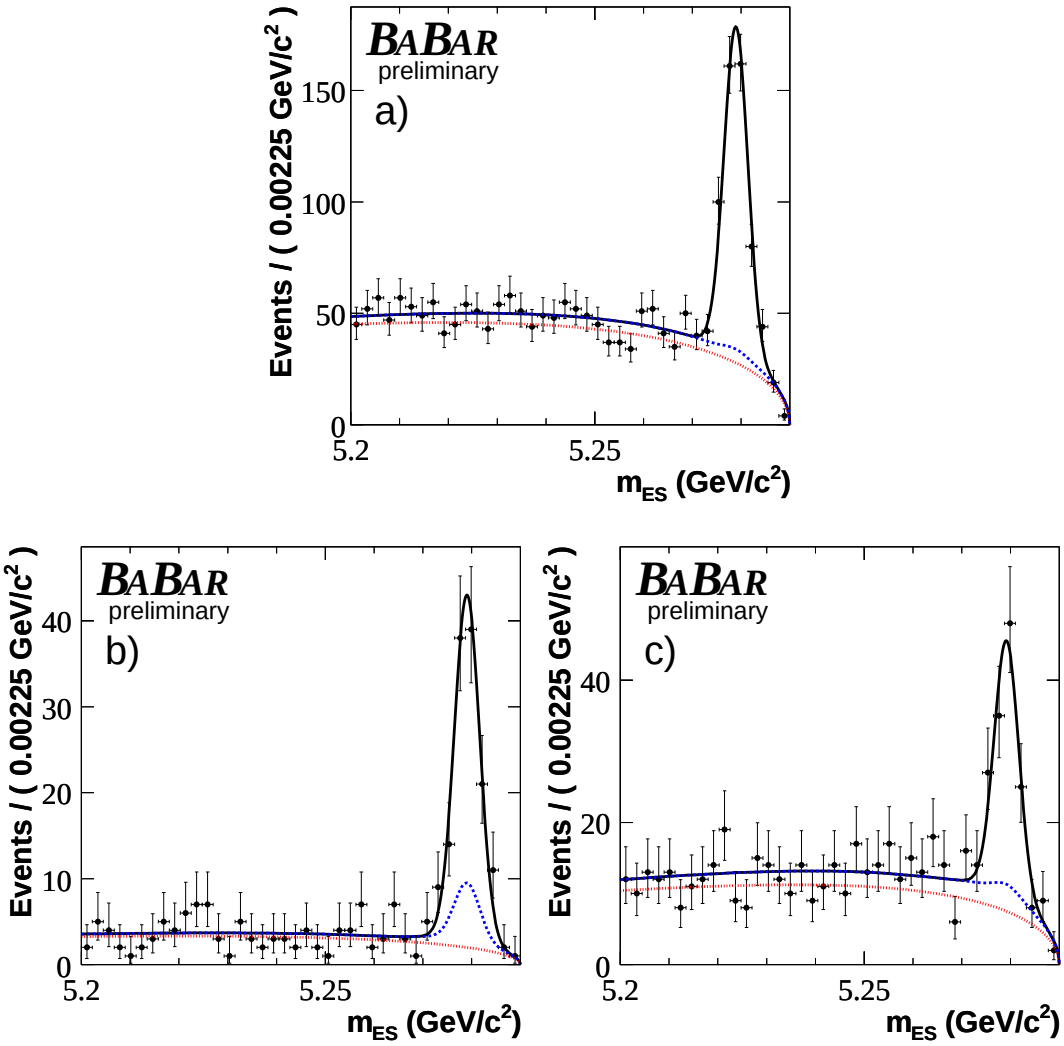

Figure 2: Distributions of $m_{\rm ES}$ for (a) $B^- \to \tilde{D}^0 K^-$, (b) $B^- \to \tilde{D}^{*0}(\tilde{D}^0\pi^0)K^-$, and (c) $B^- \to \tilde{D}^{*0}(\tilde{D}^0\gamma)K^-$. The curves superimposed represent the overall fit projections (solid black lines), the continuum contribution (dotted red lines), and the sum of all background components (dashed blue lines).

The possible absence of the σ and σ' resonances is considered in the evaluation of the systematic errors. In this respect, the K-matrix formalism [18] provides a direct way of imposing the unitarity constraint that is not guaranteed in the case of the BW model and is suited to the study of broad and overlapping resonances in multi-channel decays. We use the K-matrix method to parameterize the $\pi\pi$ S-wave states, avoiding the need to introduce the two σ scalars. A description of this alternative model can be found in [9].

Component	$Re\{a_r e^{i\phi_r}\}$	$Im\{a_r e^{i\phi_r}\}$	Fit fraction (%)
$K^*(892)^-$	-1.223 ± 0.011	1.3461 ± 0.0096	58.1
$K_0^*(1430)^-$	-1.698 ± 0.022	-0.576 ± 0.024	6.7
$K_2^*(1430)^-$	-0.834 ± 0.021	0.931 ± 0.022	3.6
$K^*(1410)^-$	-0.248 ± 0.038	-0.108 ± 0.031	0.1
$K^*(1680)^-$	-1.285 ± 0.014	0.205 ± 0.013	0.6
$K^*(892)^+$	0.0997 ± 0.0036	-0.1271 ± 0.0034	0.5
$K_0^*(1430)^+$	-0.027 ± 0.016	-0.076 ± 0.017	0.0
$K_2^*(1430)^+$	0.019 ± 0.017	0.177 ± 0.018	0.1
$\rho(770)$	1	0	21.6
$\omega(782)$	-0.02194 ± 0.00099	0.03942 ± 0.00066	0.7
$f_2(1270)$	-0.699 ± 0.018	0.387 ± 0.018	2.1
$\rho(1450)$	0.253 ± 0.038	0.036 ± 0.055	0.1
Non-resonant	-0.99 ± 0.19	3.82 ± 0.13	8.5
$f_0(980)$	0.4465 ± 0.0057	0.2572 ± 0.0081	6.4
$f_0(1370)$	0.95 ± 0.11	-1.619 ± 0.011	2.0
σ	1.28 ± 0.02	0.273 ± 0.024	7.6
σ'	0.290 ± 0.010	-0.0655 ± 0.0098	0.9

Table 1: Complex amplitudes $a_r e^{i\phi_r}$ and fit fractions of the different components ($K_S\pi^-$, $K_S\pi^+$, and $\pi^+\pi^-$ resonances) obtained from the fit of the $D^0 \to K_S\pi^-\pi^+$ Dalitz distribution from $D^{*+} \to D^0\pi^+$ events. Errors are statistical only. Masses and widths of all resonances are taken from [13] with the exception of $K_0^*(1430)^+$ taken from [16]. The fit fraction is defined for the resonance terms as the integral of $a_r^2|\mathcal{A}_r(m_-^2, m_+^2)|^2$ over the Dalitz plane divided by the integral of $|\mathcal{A}_D(m_-^2, m_+^2)|^2$. The sum of fit fractions is 119.5%. A value different from 100% is a consequence of the interference among the amplitudes.

5 CP ANALYSIS

We simultaneously fit the $B^\mp \to \tilde{D}^{(*)0}K^\mp$ samples using an unbinned extended maximum-likelihood fit to extract the *CP*-violating parameters $x_\mp^{(*)}$ and $y_\mp^{(*)}$ along with the signal and background yields. The fit uses $m_{\rm ES}$, ΔE, $\mathcal{F}$, and $m_\mp^2$. The likelihood for candidate j is obtained by summing the product of the event yield N_c, the probability density functions (PDF's) for the kinematic and event shape variables $\mathcal{P}_c$, and the Dalitz distributions $\mathcal{P}_c^{\rm Dalitz}$, over the signal and background components c. The likelihood function is

$$\mathcal{L} = \exp\left(-\sum_c N_c\right) \prod_j \sum_c N_c \mathcal{P}_c(\vec{\xi}_j)\mathcal{P}_c^{\rm Dalitz}(\vec{\eta}_j) \ , \tag{3}$$

where $\vec{\xi}_j = \{m_{\rm ES}, \Delta E, \mathcal{F}\}_j$, $\vec{\eta}_j = (m_-^2, m_+^2)_j$, and $\mathcal{P}_c(\vec{\xi}) = \mathcal{P}_{1,c}(m_{\rm ES})\mathcal{P}_{2,c}(\Delta E)\mathcal{P}_{3,c}(\mathcal{F})$. The background components in the fit are continuum, $B\overline{B}$ and $B^- \to D^0\pi^-$ (for $B^- \to D^0K^-$) or $B^- \to D^{*0}\pi^-$ (for $B^- \to D^{*0}K^-$). For signal events, $\mathcal{P}_c^{\rm Dalitz}(\vec{\eta})$ is given by $\Gamma_\mp^{(*)}(\vec{\eta})$ multiplied by the efficiency variations estimated using simulated signal events, where $\Gamma_\mp^{(*)}(\vec{\eta})$ is given by Eq. (1).

The $m_{\rm ES}$ and ΔE distributions for signal events are described by Gaussian functions; the Fisher distribution is parameterized with two Gaussian functions with different widths for the left and

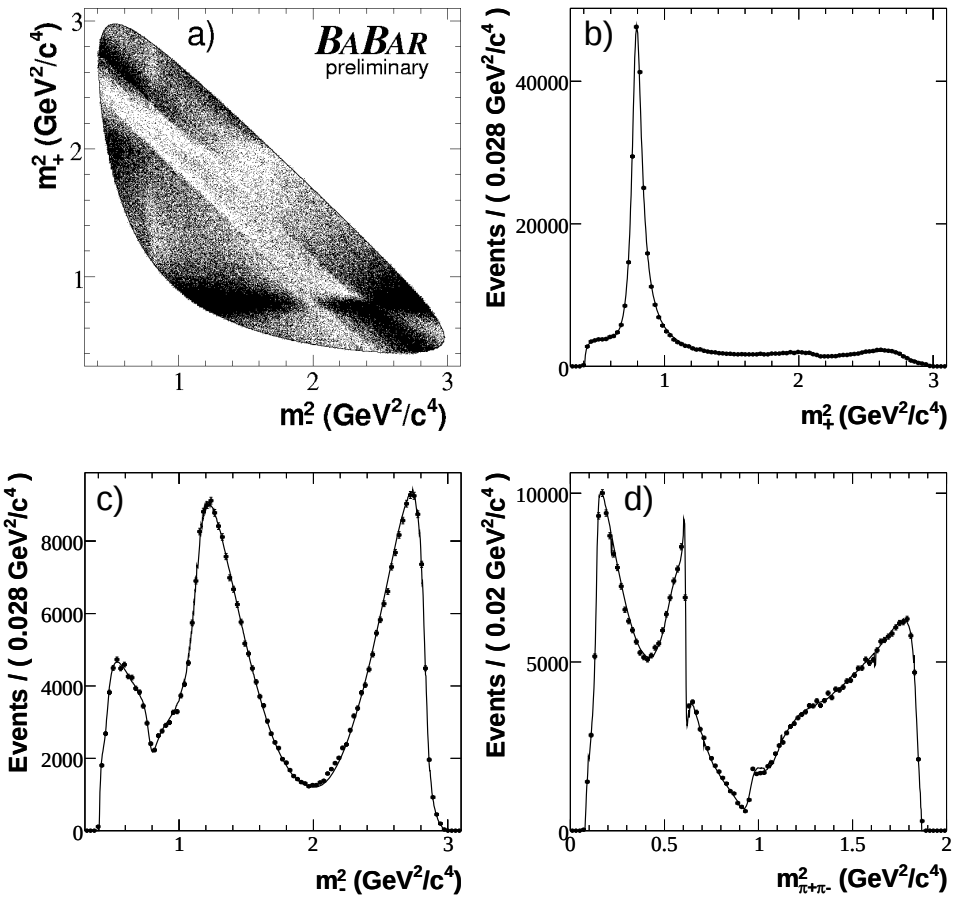

Figure 3: (a) The $\bar{D}^0 \to K^0_S\pi^-\pi^+$ Dalitz distribution from $D^{*-} \to \bar{D}^0\pi^-$ events, and projections on (b) $m^2_+ = m^2_{K^0_S\pi^+}$, (c) $m^2_- = m^2_{K^0_S\pi^-}$, and (d) $m^2_{\pi^+\pi^-}$. $D^0 \to K^0_S\pi^+\pi^-$ from $D^{*+} \to D^0\pi^+$ events are also included. The curves are the reference model fit projections.

right parts of the curve (*bifurcated Gaussian*). Their parameters, along with most of the parameters describing the background distributions, are determined from a combined fit to the $B^- \to D^{(*)0}\pi^-$ high-statistics control samples.

5.1 Description of the background probability density functions

The continuum background in the $m_{\rm ES}$ distribution is described by a threshold function [19] whose free parameter ζ is determined from the $B^- \to D^{(*)0}\pi^-$ control samples. The continuum ΔE distribution is described by a first order polynomial whose slope is extracted from the control samples. The shape of the background $m_{\rm ES}$ distribution in generic $B\overline{B}$ decays is taken from simulated events and uses a threshold function to describe the combinatorial component plus a bifurcated Gaussian shape to parameterize the peaking contribution. The fraction of the peaking contribution is extracted directly from the fit to the data. The ΔE distribution for $B\overline{B}$ background is taken from simulation and parameterized with the sum of a second order polynomial and a Gaussian function that takes into account the increase of combinatorial feed-down background at

negative ΔE values. The $m_{\rm ES}$ distribution of $B^- \to D^{(*)0}\pi^-$ is the same as the signal, while the ΔE shape is parameterized with the same Gaussian function as the signal with an additional shift arising from the wrong mass assignment to the prompt track, computed event by event as a function of the prompt track momentum in laboratory frame and the CM boost. The Fisher PDF for continuum background is determined from the $m_{\rm ES}$ sideband region of the control sample events and is parameterized with the sum of two Gaussian functions. The Fisher PDF for $B\overline{B}$ events and $B^- \to D^{(*)0}\pi^-$ background is taken to be the same as that for the signal, consistent with the simulation.

Background events arising from continuum and $B\overline{B}$ where the D^0 candidate is real can mimic either the $b \to c$ or the $b \to u$ signal component, depending on whether the D^0 candidate is combined with a negatively or positively-charged kaon. We take this effect into account in the likelihood function with two parameters, the fraction f_{D^0} of background events with a real D^0 and the fraction R of background events with a real D^0 associated with a negatively-charged kaon (same charge correlation as the $b \to c$ signal component). These fractions have been estimated separately for continuum and $B\overline{B}$ backgrounds from simulated events. As a check of the reliability of these estimates, the fraction f_{D^0} for all background events (mixture of continuum and $B\overline{B}$) has been measured on data from the invariant mass distribution of D^0 after removing the requirement on the D^0 mass and using events satisfying $m_{\rm ES} < 5.272\,{\rm GeV}/c^2$. The measured value is consistent with the fraction found on simulated events. The fractions f_{D^0} and R for continuum and $B\overline{B}$ background are reported in Table 2.

The shape of the Dalitz plot distribution of the continuum and $B\bar{B}$ background is parameterized by a third-order polynomial function in (m_-^2,m_+^2) for the combinatorial component (fake neutral D mesons), and as signal D^0 or $\bar{D}^0$ shapes for real neutral D mesons. The combinatorial distributions are taken from simulated events. The shapes for events in the D^0 invariant mass and $m_{\rm ES}$ sidebands on data and simulated events are found to be consistent. The fraction of background originating from signal $B^- \to \tilde{D}^{(*)0}K^-$ where the $\tilde{D}^{(*)0}$ meson is combined with a combinatorial (either opposite- or same-charged) kaon from the other B meson is found to be negligible.

D^0 fraction	$B^- \to \tilde{D}^0 K^-$	$B^- \to \tilde{D}^{*0}(\tilde{D}^0\pi^0)K^-$	$B^- \to \tilde{D}^{*0}(\tilde{D}^0\gamma)K^-$
f_{D^0} (continuum)	0.022 ± 0.010	0.336 ± 0.038	0.163 ± 0.016
R (continuum)	0.164 ± 0.018	0.170 ± 0.052	0.099 ± 0.031
f_{D^0} ($B\overline{B}$)	0.026 ± 0.008	0.130 ± 0.041	0.152 ± 0.024
R ($B\overline{B}$)	0.64 ± 0.15	0.5 ± 0.5	0.943 ± 0.039

Table 2: D^0 fractions f_{D^0} and R, as described in the text, from simulated continuum and $B\overline{B}$ background events.

5.2 *CP* parameters

The signal yields measured with the *CP* fit on the sample of 347 million $B\overline{B}$ events are $N(B^\mp \to \tilde{D}^0 K^\mp) = 398 \pm 23$, $N(B^\mp \to \tilde{D}^{*0}(\tilde{D}^0\pi^0)K^\mp) = 97 \pm 13$, $N(B^\mp \to \tilde{D}^{*0}(\tilde{D}^0\gamma)K^\mp) = 93 \pm 12$, and are consistent with expectations based on measured branching fractions and efficiencies estimated from Monte Carlo simulation. The results for the *CP*-violating parameters $x_\mp^{(*)}$, $y_\mp^{(*)}$ are summarized in Table 3. The only non-zero statistical correlations involving the *CP* parameters are for the pairs (x_-, y_-), (x_+, y_+), (x_-^*, y_-^*), and (x_+^*, y_+^*), which amount to -1%, 1%, -17%, and -14%,

respectively. The Dalitz plot distributions for the events selected with $m_{\rm ES} > 5.272\,{\rm GeV}/c^2$ are shown in Fig. 4 separately for B^- and B^+ candidates. Fig. 5 shows the one- and two-standard deviation confidence-level contours (including statistical and systematic uncertainties) in the $x^{(*)} - y^{(*)}$ planes for all the reconstructed modes, and separately for B^- and B^+. The separation of the $(x_-^{(*)}, y_-^{(*)})$ and $(x_+^{(*)}, y_+^{(*)})$ confidence contours in these planes is an indication of direct *CP* violation.

CP parameter	$B^\mp \to \tilde{D}^{(*)0} K^\mp$
x_-	$0.041 \pm 0.059 \pm 0.018 \pm 0.011$
y_-	$0.056 \pm 0.071 \pm 0.007 \pm 0.023$
x_+	$-0.072 \pm 0.056 \pm 0.014 \pm 0.029$
y_+	$-0.033 \pm 0.066 \pm 0.007 \pm 0.018$
x_-^*	$-0.106 \pm 0.091 \pm 0.020 \pm 0.009$
y_-^*	$-0.019 \pm 0.096 \pm 0.022 \pm 0.016$
x_+^*	$0.084 \pm 0.088 \pm 0.015 \pm 0.018$
y_+^*	$0.096 \pm 0.111 \pm 0.032 \pm 0.017$

Table 3: *CP*-violating parameters $x_\mp^{(*)}$, $y_\mp^{(*)}$ obtained from the *CP* fit to the $B^\mp \to \tilde{D}^{(*)0} K^\mp$ samples. The first error is statistical, the second is experimental systematic uncertainty and the third is the systematic uncertainty associated with the Dalitz model.

5.3 Systematic error associated with the D^0 Dalitz model

The largest single contribution to the systematic uncertainties in the *CP* parameters comes from the choice of the Dalitz model used to describe the $D^0 \to K^0_S\pi^-\pi^+$ decay amplitude. The D^0 sample used to determine the reference model introduced in Sec. 4 is fitted with a set of alternative models where the resonances are described with different parameterizations or removed:

1) $\pi\pi$ S-wave: the reference model uses two wide BW scalar amplitudes (σ and σ'). Alternatively we use a K-matrix model [9] with pole masses and coupling constants fixed by fits to scattering data [20]. See also Sec. 4.

2) $\pi\pi$ P-wave: the mass and the width of the Gounaris-Sakurai BW describing the $\rho(770)$ are changed within their quoted uncertainty [13].

3) $\pi\pi$ and $K\pi$ D-waves: alternative to the helicity formalism used in the reference model, for $f_2(1270)$ and $K_2^*(1430)$ we use the formalism derived from Zemach tensors [21]. The difference is very small for P-waves but is larger for D-waves.

4) $K\pi$ S-wave: the mass and width of the BW describing $K^*(1430)$ are taken from E791 [16]. Alternatively, we have floated them in our flavor tagged D^0 sample obtaining consistent values. As an additional model we use an adaptation of the LASS parameterization [22] with parameters taken from the fit to our $D^{*+} \to D^0\pi^+$ data sample.

5) $K\pi$ P-wave: it is dominated by the $K^*(892)$ in both Cabibbo allowed and doubly Cabibbo suppressed amplitude. The mass and the width of this resonance, taken from PDG [13] in the reference model, are changed to the values found by keeping them floating in the fit to

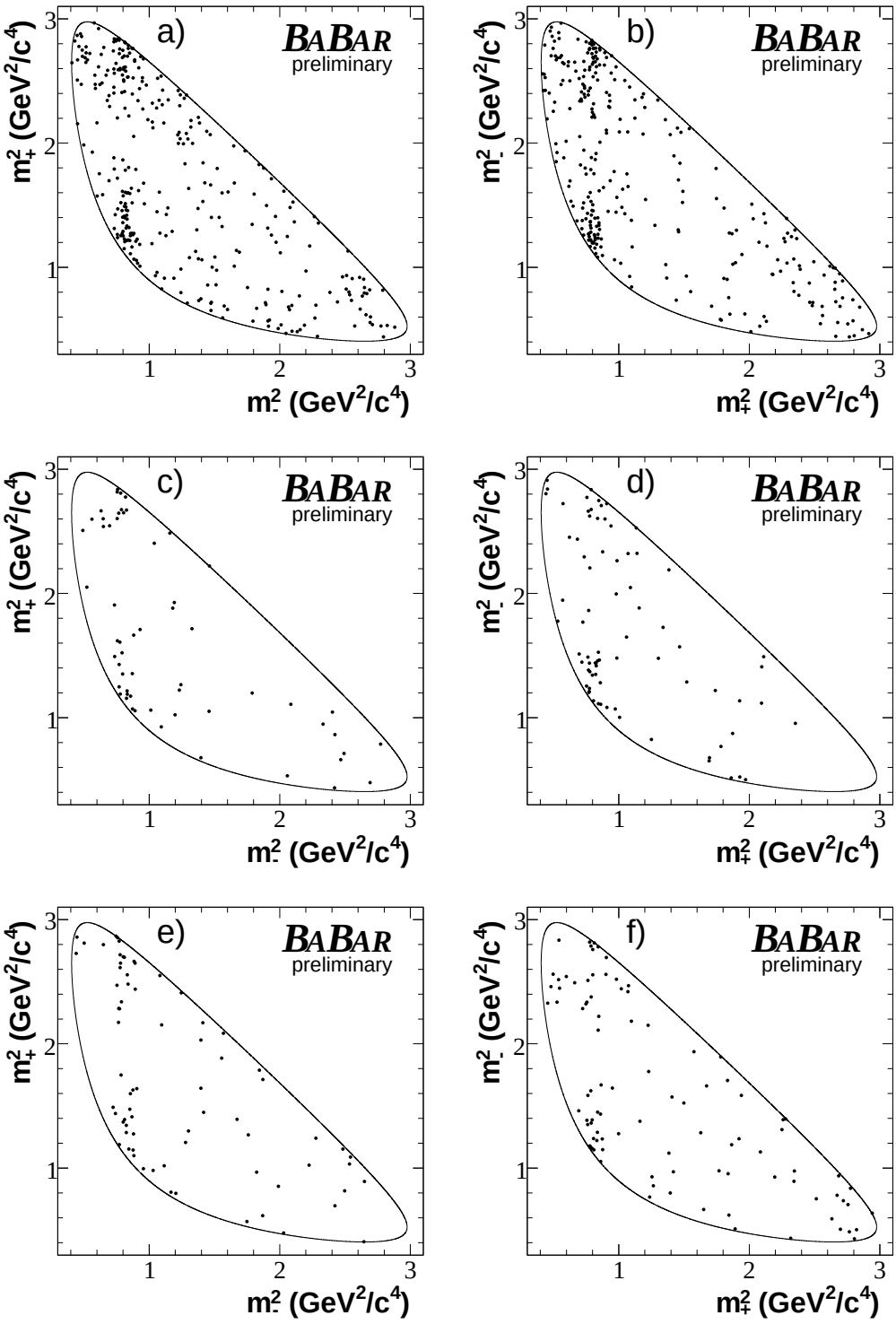

Figure 4: The $\tilde{D}^0 \to K^0_S\pi^-\pi^+$ Dalitz distributions for $B^\mp \to \tilde{D}^0 K^\mp$ (a,b), $B^\mp \to \tilde{D}^{*0}(\tilde{D}^0\pi^0)K^\mp$ (c,d), and $B^\mp \to \tilde{D}^{*0}(\tilde{D}^0\gamma)K^\mp$ (e,f), separately for B^- (a,c,e) and B^+ (b,d,f). The requirements $m_{\rm ES} > 5.272$ GeV/c^2 and $|\Delta E| < 30$ MeV have been applied to reduce the background contamination.

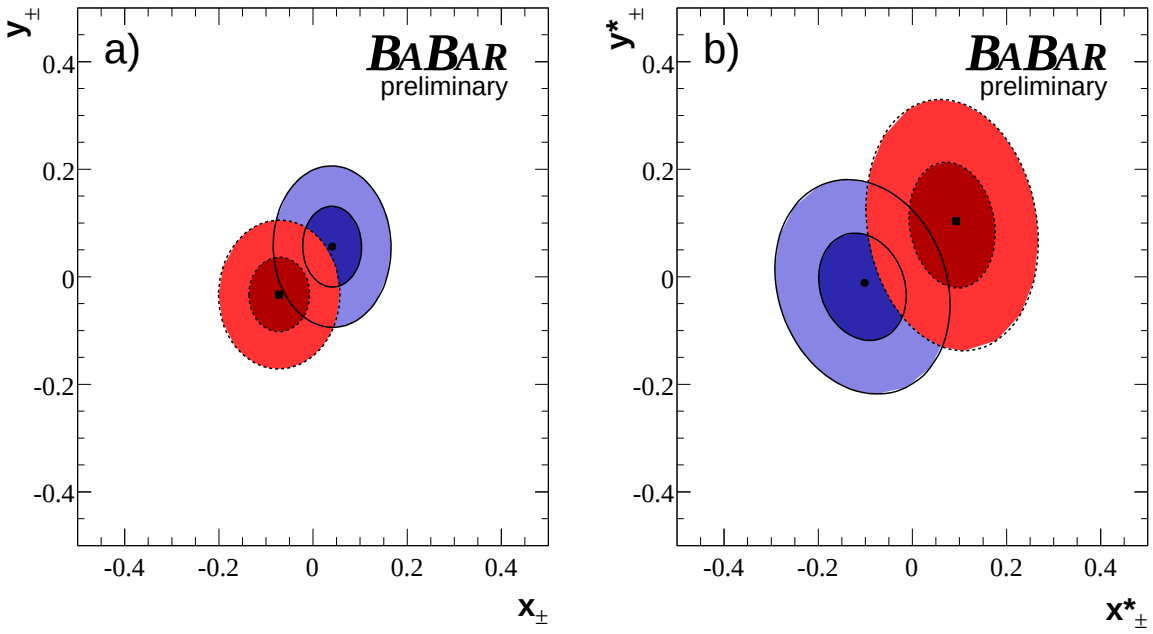

Figure 5: Contours at 39.3% (dark) and 86.5% (light) confidence level (corresponding to two-dimensional one- and two-standard deviaton regions), including statistical and systematic uncertainties, for the $(x_{\mp}^{(*)}, y_{\mp}^{(*)})$ parameters for B^- (thick and solid lines) and B^+ (thin and dotted lines) decays.

the flavour-tagged D^0 sample. The resulting values are consistent with what is found in $B \to J/\Psi K\pi$ decays selected in *BABAR* data.

6) Blatt-Weisskopf penetration factors: the effect from the Blatt-Weisskopf penetration factors has been evaluated using an alternative model that doesn't include them [23].

7) Running width of BW: a model with BW's of fixed width is used.

8) $K_2^*(1430)$, $K^*(1680)$, $K^*(1410)$ and $\rho(1450)$: these resonances are removed from the reference model.

We have generated a sample of $B^{\mp} \to \tilde{D}^0 K^{\mp}$ and $B^{\mp} \to \tilde{D}^{*0} K^{\mp}$ signal events that is one hundred times larger than the measured signal yields in data. The Dalitz plot distribution of D^0 is generated according to the reference model and to *CP* parameters consistent with the values found in data. The *CP* parameters are extracted by fitting the generated Dalitz plot distributions using a PDF equal to the reference model (*model 0*) or to one of the eight alternative models (*model 1, 2,...,8*). We take as the systematic uncertainty of $(x_{\mp}, y_{\mp})$ — similarly for $(x^*_{\mp}, y^*_{\mp})$ — associated with the i^{th} alternative model the difference between the *CP* parameters fitted using the alternative model $(x^i_{\mp}, y^i_{\mp})$ and the reference model $(x^0_{\mp}, y^0_{\mp})$: $\Delta x^i_{\mp} = x^i_{\mp} - x^0_{\mp}$, $\Delta y^i_{\mp} = y^i_{\mp} - y^0_{\mp}$. As total systematic uncertainty associated with the Dalitz model we consider the sum square of contributions from the alternative models: $\Delta x_{\mp} = \sqrt{\sum_{i=1}^{8} \Delta x^{i\,2}_{\mp}}$, $\Delta y_{\mp} = \sqrt{\sum_{i=1}^{8} \Delta y^{i\,2}_{\mp}}$. The dominant contributions

to the overall Dalitz model uncertainty arise from the models 1), 4), and 7). The systematic uncertainties associated with the Dalitz model are summarized in Table 4.

Source	x_-	y_-	x_+	y_+	x_-^*	y_-^*	x_+^*	y_+^*
$m_{\rm ES}$, ΔE, $\mathcal{F}$ shapes	0.002	0.004	0.003	0.004	0.011	0.012	0.008	0.008
Real D^0 fractions	0.002	0.000	0.000	0.000	0.002	0.003	0.002	0.016
Fraction of right sign D^0's	0.008	0.002	0.002	0.002	0.005	0.005	0.001	0.022
Efficiency in the Dalitz plot	0.014	0.000	0.013	0.001	0.001	0.002	0.000	0.001
Background Dalitz shape	0.006	0.003	0.001	0.004	0.012	0.015	0.009	0.009
Dalitz amplitudes and phases	0.004	0.004	0.004	0.004	0.008	0.008	0.008	0.008
$B^- \to D^{*0}K^-$ cross-feed	0.000	0.000	0.000	0.000	0.004	0.001	0.004	0.004
CP violation in $D\pi$ and $B\overline{B}$ bkg	0.000	0.000	0.000	0.000	0.005	0.002	0.002	0.005
Total experimental	0.018	0.007	0.014	0.007	0.020	0.022	0.015	0.032
D^0 Dalitz model	0.011	0.023	0.029	0.018	0.009	0.016	0.018	0.017
Total	0.021	0.024	0.032	0.019	0.021	0.027	0.023	0.036

Table 4: Summary of the main contributions to the systematic error on the *CP* parameters $x_\mp$, $y_\mp$, $x_\mp^*$, and $y_\mp^*$.

5.4 Experimental systematic errors

The main experimental systematic errors are listed in Table 4. Uncertainties due to the $m_{\rm ES}$, ΔE, and $\mathcal{F}$ PDF parameters for signal and background extracted from the combined fit to the $B^- \to D^{(*)0}\pi^-$ control samples (fixed in the reference *CP* fit) are estimated from the statistical differences on $x_\mp^{(*)}$ and $y_\mp^{(*)}$ when the former set of parameters is also floated in the *CP* fit. Other $m_{\rm ES}$, ΔE, and $\mathcal{F}$ parameters fixed in the *CP* fit are changed by one standard deviation. The uncertainties associated to the knowledge of the fraction of background events with a real D^0 and the Dalitz distribution of background events are evaluated from the differences on the *CP* parameters when the estimates obtained from simulated events are replaced by the estimates using sideband data. The systematic uncertainty on the fraction of events where a true D^0 is associated with a negatively-charged kaon is obtained from the variation of the *CP* parameters when the D^0 is randomly associated either to a negatively- or positively-charged kaon (absence of charge correlation). The effect due to reconstruction efficiency variations of the signal across the Dalitz plane has been estimated assuming a perfectly uniform efficiency. The statistical errors in the Dalitz amplitudes and phases from the fit to the tagged D^0 sample have been propagated to the $x_\mp^{(*)}$ and $y_\mp^{(*)}$ parameters performing a simultaneous *CP* and Dalitz fit to the $B^- \to D^{(*)0}K^-$ and $D^{*+} \to D^0\pi^+$ data. The effect of the remaining cross-feed of $B^- \to \tilde{D}^{*0}(D^0\pi^0)K^-$ events into the $B^- \to \tilde{D}^{*0}(D^0\gamma)K^-$ sample (5% of the signal yield) has been evaluated by including an additional background component with $\mathcal{P}_c^{\rm Dalitz}(\vec{\eta})$ identical to that of $B^- \to \tilde{D}^{*0}(D^0\pi^0)K^-$ signal events. Finally, possible *CP*-violating effects in the background have been evaluated by setting the *CP* parameters of the $B^- \to D^{(*)0}\pi^-$ background component to the values obtained from a *CP* fit to the $B^- \to D^{(*)0}\pi^-$ control samples, and by floating an independent set of *CP* parameters for the other $B\overline{B}$ background.

The following sources of uncertainty are found to be negligible: the assumption of perfect mass resolution for the Dalitz plot variables (m_-^2, m_+^2), the presence of combinatorial background from

signal events where the prompt kaon is replaced by a combinatorial track, and the assumption that the shape of the continuum or $B\overline{B}$ background does not change when the D^0 is fake or real.

6 INTERPRETATION

A frequentist (Neyman) procedure [13, 24] identical to that used in our previous measurements [8, 9] has been adopted to interpret the measurement of the *CP* parameters $(x_{\mp}^{(*)}, y_{\mp}^{(*)})$ reported in table 3 in terms of confidence regions on $\mathbf{p} = (\gamma, r_B, \delta_B, r_B^*, \delta_B^*)$. Using a large number of pseudo-experiments with probability density functions and parameters as obtained from the fit to the data but with many different values of the *CP* parameters, we construct a multivariate Gaussian parameterization of the PDF of $(x_{\mp}^{(*)}, y_{\mp}^{(*)})$ as a function of $\mathbf{p}$ which takes into account the statistical and systematic correlations. For a given $\mathbf{p}$, the five-dimensional confidence level $\mathcal{C} = 1 - \alpha$ is calculated by integrating over all points in the fit parameter space closer (larger PDF) to $\mathbf{p}$ than the fitted data values. The one- (two-) standard deviation region of the *CP* parameters is defined as the set of $\mathbf{p}$ values for which α is smaller than 3.7% (45.1%). Figure 6 shows the two-dimensional projections onto the $r_B - \gamma$ and $r_B^* - \gamma$ planes, including statistical and systematic uncertainties. The figure shows that this Dalitz analysis has a two-fold ambiguity, $(\gamma, \delta_B^{(*)}) \rightarrow (\gamma + 180^\circ, \delta_B^{(*)} + 180^\circ)$, as expected from Eq. (1). From the one-dimensional projections we obtain for the weak phase $\gamma = (92 \pm 41 \pm 11 \pm 12)^\circ$, and for the strong phase differences $\delta_B = (118 \pm 63 \pm 19 \pm 36)^\circ$ and $\delta_B^* = (-62 \pm 59 \pm 18 \pm 10)^\circ$. No constraints on the phases are achieved at two standard deviation level and beyond. Similarly, for the magnitude of the ratio of decay amplitudes r_B and r_B^* we obtain the one (two) standard deviations constraints $r_B < 0.140$ ($r_B < 0.195$) and $0.017 < r_B^* < 0.203$ ($r_B^* < 0.279$). All these results are obtained considering the statistical correlations mentioned in Sec. 5.2, while the experimental and Dalitz model systematic uncertainties are taken uncorrelated. We have verified that accounting for experimental systematic correlations within a given measurement $(x_{\mp}, y_{\mp})$ or $(x_{\mp}^*, y_{\mp}^*)$, or assuming the experimental and Dalitz model systematic uncertainties between $(x_{\mp}, y_{\mp})$ and $(x_{\mp}^*, y_{\mp}^*)$ fully correlated, has a negligible effect on the results.

7 CONCLUSIONS

We have presented a preliminary updated measurement of the *CP* parameters $(x_{\mp}, y_{\mp})$ and $(x_{\mp}^*, y_{\mp}^*)$ with $B^{\mp} \rightarrow \tilde{D}^{(*)0} K^{\mp}$, $\tilde{D}^{*0} \rightarrow \tilde{D}^0 \pi^0, \tilde{D}^0 \gamma$, $\tilde{D}^0 \rightarrow K_S^0 \pi^- \pi^+$ decays based on a data sample of 347 million $B\overline{B}$ pairs, that supersedes the previous one based on about 227 million $B\overline{B}$ pairs [8]. The current analysis reduces the experimental systematic uncertainty and improves the procedure to estimate the error associated with the Dalitz model of the D^0 decay.

Despite the improved measurement of $(x_{\mp}^{(*)}, y_{\mp}^{(*)})$, the uncertainty on γ has increased with respect to our previous measurement [8], moving from $\gamma = (70 \pm 31^{+12+14}_{-10-11})^\circ$ to $\gamma = (92 \pm 41 \pm 11 \pm 12)^\circ$. Since the uncertainty on γ scales roughly as $1/r_B^{(*)}$, this change is explained by noticing that the new $(x_{\mp}^{(*)}, y_{\mp}^{(*)})$ measurement favors values of $r_B^{(*)}$ smaller than our previous analysis and significantly smaller than the latest Belle results [10].

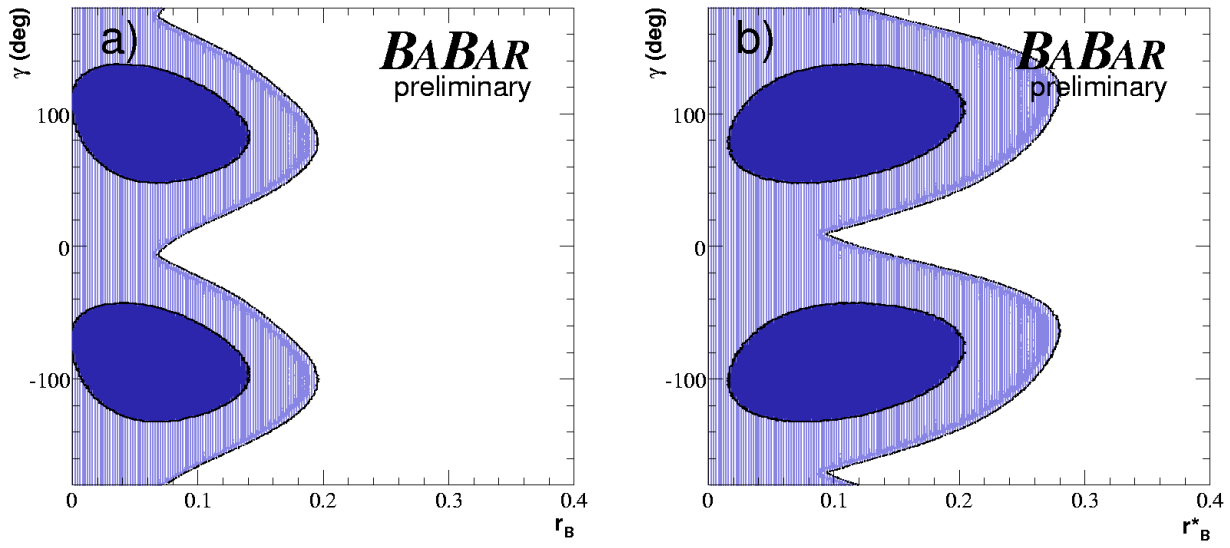

Figure 6: Projections in the (a) $r_B - \gamma$ and (b) $r_B^* - \gamma$ planes of the five-dimensional one- (dark) and two- (light) standard deviation regions.

8 ACKNOWLEDGMENTS

We are grateful for the extraordinary contributions of our PEP-II colleagues in achieving the excellent luminosity and machine conditions that have made this work possible. The success of this project also relies critically on the expertise and dedication of the computing organizations that support *BABAR*. The collaborating institutions wish to thank SLAC for its support and the kind hospitality extended to them. This work is supported by the US Department of Energy and National Science Foundation, the Natural Sciences and Engineering Research Council (Canada), Institute of High Energy Physics (China), the Commissariat à l'Energie Atomique and Institut National de Physique Nucléaire et de Physique des Particules (France), the Bundesministerium für Bildung und Forschung and Deutsche Forschungsgemeinschaft (Germany), the Istituto Nazionale di Fisica Nucleare (Italy), the Foundation for Fundamental Research on Matter (The Netherlands), the Research Council of Norway, the Ministry of Science and Technology of the Russian Federation, Ministerio de Educación y Ciencia (Spain), and the Particle Physics and Astronomy Research Council (United Kingdom). Individuals have received support from the Marie-Curie IEF program (European Union) and the A. P. Sloan Foundation.

References

[1] N. Cabibbo, Phys. Rev. Lett. **10**, 531 (1963);
M. Kobayashi and T. Maskawa, Prog. Theor. Phys. **49**, 652 (1973).

[2] L. Wolfenstein, Phys. Rev. Lett. **51**, 1945 (1983).

[3] Reference to the charge-conjugate state is implied here and throughout the text unless otherwise specified.

[4] M. Gronau and D. London, Phys. Lett. B **253**, 483 (1991); M. Gronau and D. Wyler, Phys. Lett. B **265**, 172 (1991);

[5] D. Atwood, I. Dunietz and A. Soni, Phys. Rev. Lett. **78**, 3257 (1997).

[6] A. Giri, Y. Grossman, A. Soffer and J. Zupan, Phys. Rev. D **68**, 054018 (2003).

[7] Belle Collaboration, A. Poluetkov *et al.*, Phys. Rev. D **70**, 072003 (2004).

[8] *BABAR* Collaboration, B. Aubert *et al.*, Phys. Rev. Lett. **95**, 121802 (2005).

[9] *BABAR* Collaboration, B. Aubert *et al.*, hep-ex/0507101.

[10] Belle Collaboration, A. Poluetkov *et al.*, Phys. Rev. D **73**, 112009 (2006).

[11] A. Bondar and T. Gershon, Phys. Rev. D **70**, 091503 (2004).

[12] *BABAR* Collaboration, B. Aubert *et al.*, Nucl. Instr. Methods Phys. Res., Sect. A **479**, 1 (2002).

[13] Particle Data Group, S. Eidelman *et al.*, Phys. Lett. B **592**, 1 (2004).

[14] G.J. Gounaris and J.J. Sakurai, Phys. Rev. Lett. **21**, 244 (1968).

[15] CLEO Collaboration, S. Kopp *et al.*, Phys. Rev. D **63**, 092001 (2001).

[16] E791 Collaboration, E. M. Aitala *et. al.*, Phys. Rev. Lett. **89**, 121801 (2002).

[17] The σ and σ' masses and widths are determined from the data. We find (in MeV/c^2) $M_\sigma = 490 \pm 6$, $\Gamma_\sigma = 406 \pm 11$, $M_{\sigma'} = 1024 \pm 4$, and $\Gamma_{\sigma'} = 89 \pm 7$. Errors are statistical.

[18] E. P. Wigner, Phys. Rev. **70**, 15 (1946); S. U. Chung *et al.*, Ann. Phys. **4**, 404 (1995); I. J. R. Aitchison, Nucl. Phys. A **189**, 417 (1972).

[19] $\frac{dN}{dm_{ES}} = N \cdot m_{\rm ES} \cdot \sqrt{1-x^2} \cdot \exp\left(-\zeta \cdot (1-x^2)\right)$ where $x = 2m_{\rm ES}/\sqrt{s}$ and the parameter ζ is determined from a fit. ARGUS Collaboration, H. Albrecht *et al.*, Z. Phys. C **48**, 543 (1990).

[20] V.V. Anisovich and A.V. Sarantsev, Eur. Phys. Jour. **A16**, 229 (2003).

[21] V. Filippini, A. Fontana and A. Rotondi, Phys. Rev. D **51**, 2247 (1995).

[22] LASS Collaboration, D. Aston *et al.*, Nucl. Phys. B **296**, 493 (1988).

[23] J. Blatt and V. Weisskopf, *Theoretical Nuclear Physics*. New York: John Wiley & Sons (1952).

[24] J. Neyman, Phil. Trans. Royal Soc. London, Series A, **236**, 333 (1937), reprinted in *A selection of Early Statistical Papers on J. Neyman* (University of California Press, Berkeley, 1967).